Diffusion of Oligomeric Species in Polymer Solutions

Mark C. Piton,† Robert G. Gilbert,*,† Bogdan E. Chapman,‡ and Phillip W. Kuchel*,‡

School of Chemistry, Sydney University, Sydney, NSW 2006, Australia, and Department of Biochemistry, Sydney University, Sydney, NSW 2006, Australia

Received January 25, 1993; Revised Manuscript Received April 21, 1993

ABSTRACT: Self-diffusion coefficients (D_s) for analogs of polystyrene (PS) oligomers were measured using pulsed field gradient (PFG) ^{1}H NMR as a function of the weight fraction (w_p) of high molecular weight PS (125000–250000) in solution over the range $0 \le w_p \le 0.6$. The studies were performed at 25 °C using benzene as solvent. Model compounds used were benzene, 1,3-diphenyl-1-butanol, and a commercially-available, monodisperse sample of PS (so-called M_5) of a peak-average molecular weight of M_p = 580 as determined by gel permeation chromatography (GPC). GPC data and PFG NMR data were used to determine a new average molecular weight for M_5 of 500. The scaling law dependence of the D_s values on the molecular weight of the model compounds was determined and a simple scaling dependence was observed with the scaling law changing linearly with w_p over the range studied. This is discussed in light of current models. D_s data are also presented for the diffusion of toluene in toluene/PS solutions over the range $0 \le w_p \le 0.7$ and are 20%–30% smaller than identical experiments reported by Pickup and Blum (see ref 13).

Introduction

A great deal of attention has recently been given to obtaining a molecular-level understanding of the factors which affect the kinetics of free-radical polymerization. Many free-radical polymerization reactions are limited by the rate at which the reactive species can diffuse together. Termination reactions are always diffusion controlled: below the critical overlap concentration (c^*), the rate-determining process is predominantly diffusion of entities within separated polymer coils. Above c^* but below the glass transition temperature, center-of-mass diffusion of small radicals limits termination, and beyond the onset of the glass transition, diffusion probably occurs by the stepwise movement of the radical end by propagative growth, a process frequently referred to as "reaction diffusion".[1-3] Shortly before the onset of glass transition, which depends on both temperature and the weight fraction of polymer in solution (w_p), reactions such as propagation and transfer (usually to monomer or another small molecule such as a transfer agent) often become diffusion controlled (when the polymer in solution slows down the diffusivity of the reactants enough that the rate of diffusive encounter between reactants competes with the rate of their chemical reaction).

The second-order rate coefficient for termination, k_t, is described by the Smoluchowski equation

$$k_t = 4\pi N_A [D_s^a + D_s^b] R \qquad (1)$$

where N_A is Avogadro's constant, the mutual-diffusion coefficient for the approach of the two reactants a and b toward one another is taken to be the sum of the individual self-diffusion coefficients D_s^a and D_s^b, and R is the "capture radius" of the reactants. In the simplest analysis, k_t depends on the degrees of polymerization i and j (or equivalently, on the molecular weight, MW) of a and b, and on w_p. R is believed to be independent of these parameters.[4,5] Consequently, the dependence of k_t on i, j, and w_p has been used in the kinetic analyses of both bulk and emulsion polymerizations.[6,7]

For detailed kinetic modeling, predictive purposes, or mechanistic interpretations of polymerization kinetics and final molecular weight distributions of polymers, one needs a quantitative estimate of $D_s(i,w_p)$.[8] Experimentally-determined data are needed for a detailed understanding of free-radical polymerization and diffusion in polymer solutions. Beyond a few percent of polymer in the solution, large polymer molecules become entangled while, up until approximately the glass transition, small chains are relatively free to diffuse. Diffusing species encounter obstructive polymer chains and are retarded; the fraction of such obstructions increases with w_p. In general, as w_p increases, diffusion decreases and with it the rate of any reactions that are sensitive to it changes. In the absence of polymer, the molecular diffusivity of a small molecule depends on the inverse square root of the molecular mass,[9] a dependence which has recently been confirmed indirectly by Amin Sanayei and O'Driscoll[10] for polystyrene (PS). As more polymer is added to the solution, this dependence becomes increasingly sensitive to the molecular weight of the diffusing species. Experimental data would, in principle, allow a test of the qualitative and quantitative aspects of current theories of the permeation of solutes in polymer lattices.

The purpose of this present work is to test scaling laws currently used for the dependence of D_s on i and w_p. To accomplish this we determined $D_s(i,w_p)$ of several oligomers of PS over a wide range of w_p. Data are presented for $D_s(1,w_p)$, and $D_s(2,w_p)$ using analogues of PS oligomers and for $\langle D_s(5,w_p) \rangle$ using a commercially available polymer standard where the brackets denote that the results are a weighted average value of D_s that takes into account the finite polydispersity index of the sample.

We used pulsed field gradient (PFG) NMR as the technique with which to determine all $D_s(i,w_p)$ values. This technique has the advantage that it allows the monitoring of the diffusion of molecules that possess values of D_s greater than *ca.* 10^{-14} m^2 s^{-1}. Such values are typical of small molecules diffusing within most polymer solutions of low w_p, above the glass transition temperature, so the method was ideally suited to our purposes. Many PFG NMR studies to monitor diffusion in polymer systems have been reported: for the diffusion of solvents in polymers (e.g. benzene,[11] cyclohexane,[11,12] and toluene[13] in PS), monomer in polymer (e.g., methyl methacrylate in poly(methyl methacrylate) (PMMA)[5]), and for polymer in polymer (e.g., PMMA in PMMA[14]). In PFG NMR

* Authors to whom correspondence should be addressed.
† School of Chemistry.
‡ Department of Biochemistry.

0024-9297/93/2226-4472$04.00/0

experiments,[15,16] the sample is placed in a static magnetic field which induces the alignment of the nuclear magnetic moments along the z-axis, thus producing a net magnetization of the sample. Application of a 90° radio frequency pulse along the x-axis rotates that magnetization into the x,y plane; it then precesses to give a decaying transverse magnetization which gives rise to the NMR signal. Application of a pulsed linear magnetic field gradient, along the z-axis, changes the precessional frequency of the nuclei as a function of their position along the gradient axis; this leads to a rapid dephasing of the macroscopic transverse magnetization and a labeling of the nuclei with a position-dependent phase angle. Application of further radio-frequency pulses and a magnetic field gradient equal to the original one can lead to complete rephasing of the macroscopic transverse magnetization vectors if the nuclei do not move. If the nuclei diffuse to some other position, they will see a different magnetic field during the application of the second gradient and will not refocus completely, leading to an attenuation of the signal,[17] and it is from this attenuation that one obtains D_s.

Experimental Section

Samples. Tracer molecules used as models for PS were both benzene (Aldrich) and toluene (Merck) for monomeric-sized species (M_1); for the dimer (M_2) 1,3-diphenyl-1-butanol was used; and the pentamer (M_5) of PS was an unfractionated, commercially-obtained (Polymer Laboratories) PS standard. M_2 was prepared by reducing 1,3-diphenyl-1-butanone (Frinton Laboratories) using $LiAlH_4$ (Aldrich) in dry diethyl ether at 20 °C (1 h) followed by protonation with MeOH. The viscous, clear, colorless compound was purified by column chromatography on silica gel (Kieselgel 60, Merck) using ethyl acetate as the eluent to provide M_2 in 92% yield. The nature of the product was confirmed by IR and NMR spectroscopies and no extraneous products were observed.

M_5 was a commercially-available (Polymer Laboratories) PS standard (MW_{peak} = 580, MW_w/MW_n < 1.14) and was used as received. M_5 was analyzed using a gel permeation chromatography (GPC) apparatus consisting of a Waters 510 HPLC pump, Waters 441 UV detector fitted with a 254 nm bandpass filter, and a Waters 100 Å μStyraGel analytical column. The sample was analyzed using THF (Merck; spectroscopic grade) as the eluent operating at ambient temperatures and at a flow rate of 0.1 mL/min. Acetone in THF, eluted under the same conditions, was used to assign the relative oligomeric peaks within the GPC chromatogram.

The majority of the samples were prepared using benzene as the solvent, with varying amounts of high-MW PS to form the polymer matrix. Samples containing PS and toluene were also prepared for the purposes of comparing our results with those in the literature.[13] Individual solutions were prepared by weighing PS (MW = 125000–250000; Polymer Laboratories), solvent (either benzene or toluene; Merck Analytical Grade), and tracer (20–30 mg) to approximately 0.5 g total. Samples were prepared in 9 mm o.d., flat-bottomed, precision NMR tubes (Wilmad) which were then sealed with Teflon® stoppers and then placed in an oven at 50–60 °C for up to 2 weeks to anneal. In the calculations of w_p, the mass of the probe was used as solvent for the M_1, and M_2. When M_5 was used as the probe, w_p was calculated using the mass of M_5 as both solvent and polymer, thereby providing a lower and upper limit to w_p, respectively, rather than a single value of w_p.

Prior to the NMR measurements, a Teflon vortex plug was inserted in the 9 mm o.d. tube to the level of the polymer solution and the entire tube inserted into a 10 mm o.d. precision tube containing CCl_4. This procedure was used to minimize the effects of magnetic susceptibility differences above and below the solution's dimensions which made shimming of the signal difficult. As well, the procedure greatly enhanced the resolution of the spectra. We observed differences in D_s for samples with and without the Teflon plugs, and the differences were due mainly to the difficulty in assigning uniquely the changes in peak intensity to the particular species of interest. With enhanced resolution arising from the use of the Teflon plugs, more precise values of D_s were obtained, which differed by up to 30% from those estimated using the less precise procedure. The position of the solution in the sample support was adjusted so that it was in the center portion of the NMR gradient coil.

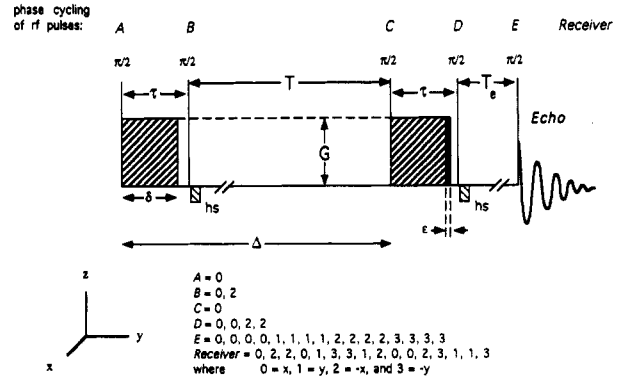

Figure 1. The LEDSTE pulse sequence. The large, positive shaded rectangles represent the diffusion gradient pulses and the smaller negative shaded rectangles represent the homospoil gradient pulses. The phase cycling of the radio-frequency pulses and receiver is given in the figure. Additional information on this pulse sequence is given by Gibbs and Johnson.[19]

NMR Analysis. The PFG NMR technique and instrumentation employed in these studies are described elsewhere.[18] Diffusion experiments were performed on a Bruker AMX-400 wide bore NMR spectrometer operating at 400.13 MHz. ^1H NMR spectra were obtained using the proton decoupling coil of a 10 mm multinuclear probe fitted with a shielded gradient coil. The *l*ongitudinal *e*ddy-current *d*elay modification to the *s*timulated-*e*cho experiment (the so-called LEDSTE pulse sequence) of Gibbs and Johnson[19] was used to obtain diffusion spectra.

The LEDSTE pulse sequence is depicted in Figure 1, together with the phase cycling used for the radio-frequency pulses, as this is not explicit in the previous reference. During the time intervals T and T_e the desired magnetization is "stored" longitudinally and homospoil gradient pulses are used to remove unwanted transverse magnetization thus giving a 16-transient phase cycle. Parameters used were as follows: τ = 30 ms, Δ = 50 or 100 ms, δ = 0–22.5 ms increased in 1.5-ms increments (in so-called "little-delta" experiments) giving 16 spectra per experiment, and T_e, a delay to allow the decay of eddy currents induced in conductive components of the probe and cryostat, was 20 ms. The magnitude of the diffusion gradients, G, was varied in the range 36–250 mT m^{-1} to give a signal attenuation of at least 90% between the first and last spectrum of the diffusion experiment. The homospoil gradients were 3 ms in duration and 120 mT m^{-1} in magnitude. A relaxation delay of 12 s was used per transient and 16 transients (one "pass" of the 16-step phase cycle) were averaged for each spectrum. At high gradient strengths it was necessary to employ an empirical correction (ϵ) to the duration of the second gradient pulse. This correction was in the microsecond range, as described by Hrovat and Wade.[20] Typical spectra are shown in Figure 2, using M_2 in toluene/PS at w_p = 0.15 to demonstrate the ability to assign selectively each molecular species.

The magnitude of the gradient pulses was calibrated as before[18] using cell imaging and secondary standards of known diffusion coefficient. Diffusion coefficients obtained for the standards at 25 °C were 2.19×10^{-9} m^2 s^{-1} for benzene (literature value[15] 2.18×10^{-9} m^2 s^{-1}), 2.26×10^{-9} m^2 s^{-1} for water (literature value[21] 2.299×10^{-9} m^2 s^{-1}), and 1.47×10^{-9} m^2 s^{-1} for cyclohexane (literature value[13] 1.47×10^{-9} m^2 s^{-1}). For large gradient settings (G > 250 mT m^{-1}), a literature value of 1.87×10^{-12} m^2 s^{-1} for glycerol[20] was used to calibrate the magnitude of the gradient.

Results

The PFG NMR spectra were all adequately resolved so that the molecules of interest could be analyzed without difficulty (see Figure 2). Signal intensities (I) were determined either by numerical integration or by manually measuring the amplitude of the peaks. The attenuation of the PFG NMR signal for a given sample, I/I_0, was

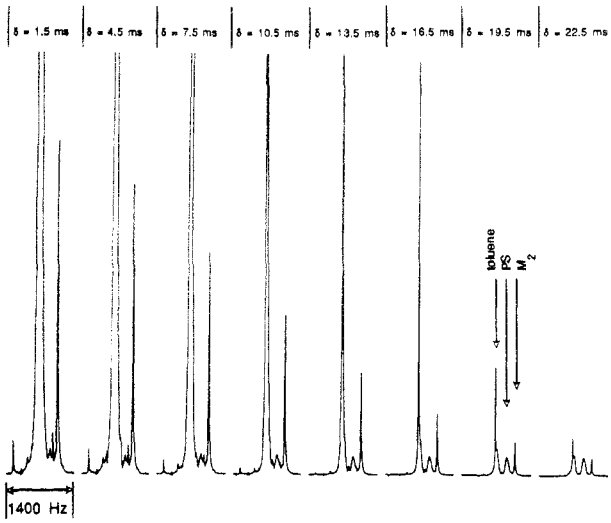

Figure 2. The alkyl region of PFG ^{1}H NMR spectra of M_2 in PS/toluene at $w_p = 0.15$ is shown as an example of the resolution possible in typical experiments. Eight spectra have been taken from 16 such spectra and the δ values have been provided in the figure. The methyl peak of the solvent has been cut off to allow the vertical expansion of the M_2 alkyl region. It can be seen from the spectra that the resolution and dynamic range of the spectra are sufficient to distinguish the tracer M_2 methyl peak from the solvent and polymer peaks.

analyzed according to the exponential equation[16]

$$\frac{I}{I_0} = \exp[-D_s(i,w_p)\, G^2\, \gamma^2\, (\delta^2(\Delta - \delta/3))] \qquad (2)$$

for the diffusion of molecules in isotropic media, where G is the magnitude of the gradient pulses, δ and Δ are the duration and time between the pulses, respectively, I is the signal intensity of the peak for a given value of δ and I_0 is magnitude of I at $\delta = 0$, and γ is the magnetogyric ratio of the nucleus of interest, ^{1}H. In the so-called "little-delta" experiments, δ was varied while keeping all other variables constant. In the fitting process, $\delta^2(\Delta - \delta/3)$ was the independent variable in the nonlinear regressions of the experimental data to expression (2) modified by the addition of a preexponential parameter which, although near 1.0, was allowed to float in the fitting procedure.

Figure 3 shows the dependence of the observed values of $D_s(i,w_p)$ for $i = 1$ and 2 and $\langle D_s(5,w_p)\rangle$ for $w_p = 0$–0.7. Also plotted are data for benzene at 25 °C (interpolated from Kosfeld and Goffloo[11]) and for toluene at 25 °C.[13] It is apparent that our data values for toluene in toluene/PS and for benzene in benzene/PS are superimposed on one another for $w_p \gtrsim 0.03$ (beyond c^* for such large PS chains as the polymer matrix). Furthermore, our data for benzene/PS are consistent with those of Kosfeld and Goffloo[11] but are smallar by 20–30% compared to those of Pickup *et al.*[13] Samples of M_2 and M_5 studied in benzene/PS are also included in Figure 3.

Discussion

The dependence of D_s on the degree of polymerization, i, is generally thought to change with w_p. In dilute solution, the diffusion coefficient depends on i (and on MW) of the diffusing species according to the simple relationship[9]

$$D_s(i,w_p \approx 0) = Ki^{-0.5} \qquad (3)$$

where K is a proportionality constant which depends on the conformation of the particular polymer. Relationship 3 appears to be surprisingly universal and has been shown to hold for small molecules diffusing in common solvents, as well as for dilute solutions of large macromolecules under their theta conditions. Interestingly, in the former case

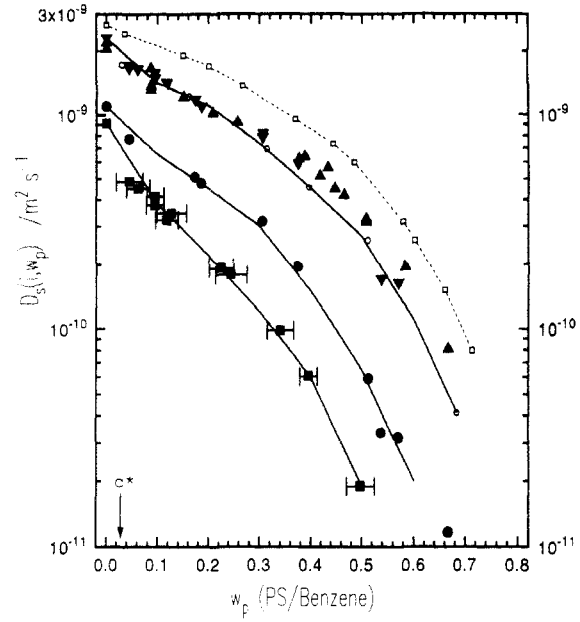

Figure 3. Experimentally-determined D_s values for analogs of PS oligomers in solutions containing PS at 25 °C as a function of w_p by PFG NMR: toluene in PS/toluene (▲), benzene in PS/benzene (▼), M_2 in PS/benzene (●), and M_5 in PS/benzene (■). Also presented are PFG NMR data from Kosfeld and Goffloo[11] for the diffusion of benzene in PS/benzene at 25 °C (○) and from Pickup *et al.* for the diffusion of toluene in PS/toluene at 25 °C (□). Lines are interpolations from which $D_s(i,w_p)$ data for Figures 6–8 were obtained. ($c^* = 0.03$ g mL^{-1} for the PS matrix ($MW_{PS} = 1.25 \times 10^5$) in benzene at 25 °C.)

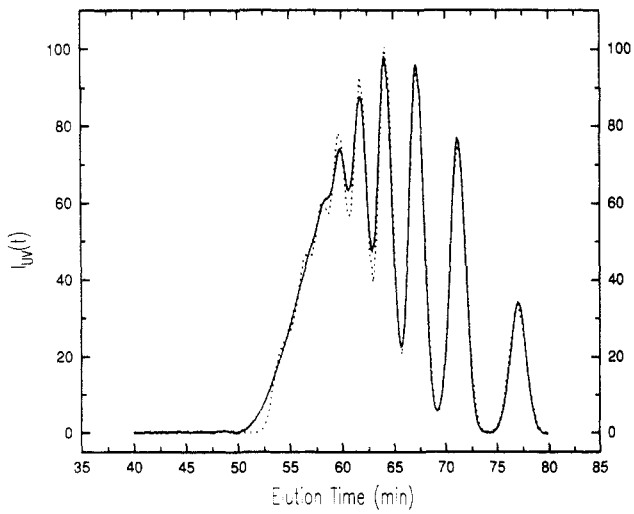

Figure 4. GPC chromatogram for a sample of M_5 in THF: experimental results (——) and results of fitting to eq 5 (– – –).

the dependence on D_s on $MW^{-0.5}$ has been reported for molecules which possess disparate structures.[22–24]

In order to determine the average, or apparent, value of MW for M_5, data from GPC coupled with that from PFG NMR were used along with the dependence in (3). GPC yielded the relative amounts of oligomeric species in the commercial sample. By use of this information and eq 3, anticipated PFG NMR signal attenuations were calculated for a sample of M_5 at $w_p = 0$. Comparison of the calculated results with those from experiment tests the assumptions involved with the GPC analysis and allowed for the calculation of an average MW for M_5 using expression 2. This procedure is given below.

Figure 4 shows the GPC chromatogram of the sample of M_5. It is apparent from the figure that at least eight oligomeric species of PS, ranging from dimer to nonamer, were present in the sample, and that most of the species were well separated. Consequently, an accurate estimate

Table I. Results of Fitting Equations 5 and 6 to the Observed GPC Data Shown in Figure 4

peak no. (n)	oligomer assign	$t_{c,n}$ (min)	w_n (min)	A_n	a_i
1	dimer	77.0	1.66	54.2 ± 4.98	27.1
2	trimer	71.2	1.54	116 ± 4.79	38.7
3	tetramer	67.2	1.48	141 ± 4.70	35.3
4	pentamer	64.2	1.35	136 ± 4.48	27.2
5	hexamer	61.8	1.35	124 ± 4.51	20.7
6	heptamer	59.8	1.35	102 ± 4.61	14.6
7	octamer	58.1	1.35	74.1 ± 4.73	9.25
8	nonamer	56.5	1.35	54.6 ± 5.24	6.06
9	decamer	55.2	1.35	24.3 ± 5.57	2.43
10	undecamer	54.0	1.35	23.6 ± 5.03	2.15

of the amount of each oligomer should therefore be possible by numerically deconvoluting the GPC trace to give the number MWD of the sample and the relative amounts of each oligomer. To account for all but a small section of the very earliest portion of the chromatogram (large i), a range of i = 2–11 was assumed and the curve was deconvoluted by fitting it to a sum of ten Gaussians using the commercial software package ORIGIN (MicroCal, Inc.; ver. 2.24). In Figure 4 indices of the peaks (n) numbered from right to left are assigned to the oligomers (i) for dimer through undecamer, respectively. Peak assignments were made based on the analysis of M_2 by GPC under identical conditions and on the information provided by the manufacturer. Fitting was performed using fixed distribution widths, fixed centers, and with only peak areas as variables. The peak positions, t_c, were determined for all ten peaks using the right-most peaks 1 through 4 and fitting their elution times as a function of the molecular weights, according to the usual GPC calibration method. Doing this for the data in Figure 4 resulted in

$$t_c = 284.7\mathrm{MW}^{-0.2343} \tag{4}$$

from which all of the remaining peak positions were determined. Values of $t_{c,n}$ used for peaks 5 to 10, calculated using eq 4 to fit the distribution, are listed in Table I. Peak widths at half height, w_n, listed in Table I, were then determined by fitting the first four peaks (1–4) to a sum of four Gaussian distributions using the peak centers determined using the above method. Widths for the remaining peaks were assumed to be identical to that of the fourth peak.

These widths and peak positions were then fixed in the fitting process as this reduced the number of variables from 30 to 10. The UV-detector signal from the GPC apparatus was recorded as a function of elution time, $I_{UV}(t)$, and the data were fitted to a function described by the sum of 10 Gaussian distributions

$$I_{UV}(t) = \left(\frac{\pi}{2}\right)^{-1/2} \sum_{n=1}^{10} \frac{A_n}{w_n} \exp\left(-\frac{2(t-t_{c,n})}{w_n^2}\right) \tag{5}$$

where A_n (variable), w_n (fixed), and $t_{c,n}$ (fixed) are the area under each Gaussian curve, its width at half height, and position of the maximum ordinate, respectively. The subscripted indices in (5) are incremented from the right-most peak in the distribution (i = 2) in Figure 4. The fitting results are listed in Table I and are shown as the dotted line in Figure 4.

Since the GPC UV detector is sensitive to the number of light-absorbing units in the polymer, and, for the detection of PS at 254 nm one may safely assume that this is identical to the number of phenyl rings on each i-mer, the relative number of chains with the degree of polymerization i is defined as a_i

$$a_i = A_n/i \tag{6}$$

From the deconvoluted GPC curve we calculated the anticipated PFG NMR signal attenuations at w_p = 0 in little-delta experiments assuming a given value of D_s for each species. Thus, three things were assumed: (a) that relationship 3 is suitable for molecules of sizes up to and including the undecamer of PS at w_p = 0; (b) that all of the molecules in the sample were derived from the n-BuLi initiator fragment and possessed the structure

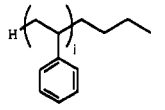

with molecular weights $\mathrm{MW}_i = 1 + i(104) + 57$ (where 57 is the n-Bu tail); (c) that $D_s(i>1,w_p=0)$ can be calculated using eq 7

$$D_s(i>1,w_p=0) = D_s(1,w_p=0)\left[\frac{\mathrm{MW}_1}{\mathrm{MW}_i}\right]^{1/2} \tag{7}$$

where the value of $D_s(1,w_p=0)$ used was that for neat benzene (MW_1 = 78, for which $D_s(1,w_p=0) = 2.31 \times 10^{-9}$ $\mathrm{m^2\ s^{-1}}$) and the individual values of MW_i were calculated assuming the structural formulas indicated above. Values of the PFG NMR attenuation I/I_0 were then calculated using the calculated values of $D_s(2\le i\le 11,w_p=0)$ in the summed version of expression 2

$$\frac{I}{I_o} = \frac{\sum_{i=2}^{11} a_i \exp[-D_s(i,w_p)\,G^2\gamma^2(\delta^2(\Delta-\delta/3))]}{\sum_{i=2}^{11} a_i} \tag{8}$$

for w_p = 0. Values of the attenuation I/I_0 predicted in this way were plotted in Figure 5 along with the experimental data obtained using identical values of G, Δ, and δ. There is a very good correspondence between the experimental and predicted (calculated) data. The apparent slopes of the lines are virtually identical. Thus despite the fact that the fitting involves a large number of parameters, the good resolution of the peaks enabled a precise determination of the value of the relative amount of each oligomer (i.e. values for each a_i).

Rearranging eq 2 provides the observed value of $\langle D_s(5,w_p=0)\rangle = 9.08 \times 10^{-10}$ $\mathrm{m^2\ s^{-1}}$ and eq 7 using benzene at 25 °C for $D_s(1,w_p=0)$ gives an average molecular weight of 500 for M_5. I/I_0 attenuations calculated using other scaling laws for D_s or using different relative a_i values give different values for $\langle D_s(5,w_p=0)\rangle$. A few of these are shown in Figure 5. While it would be ideal to have several molecular weights with which to test the dependence of D_s on MW at higher w_p, three oligomers allowed us to perform a semiquantitative empirical analysis.

At higher w_p beyond c^*, where the elevated concentration of polymer results in entanglement of the chains, the power law exponent that relates D_s to MW is believed to change from –0.5 to –1.[25] This has been expressed in terms of D_s for the monomer (i = 1) as[3]

$$D_s(i,w_p) = \frac{D_s(1,w_p)}{i} \tag{9}$$

$$i < X_c$$

where X_c is a critical length of the diffusing species. For $i \ge X_c$, it was suggested[3] that D_s is much more sensitive

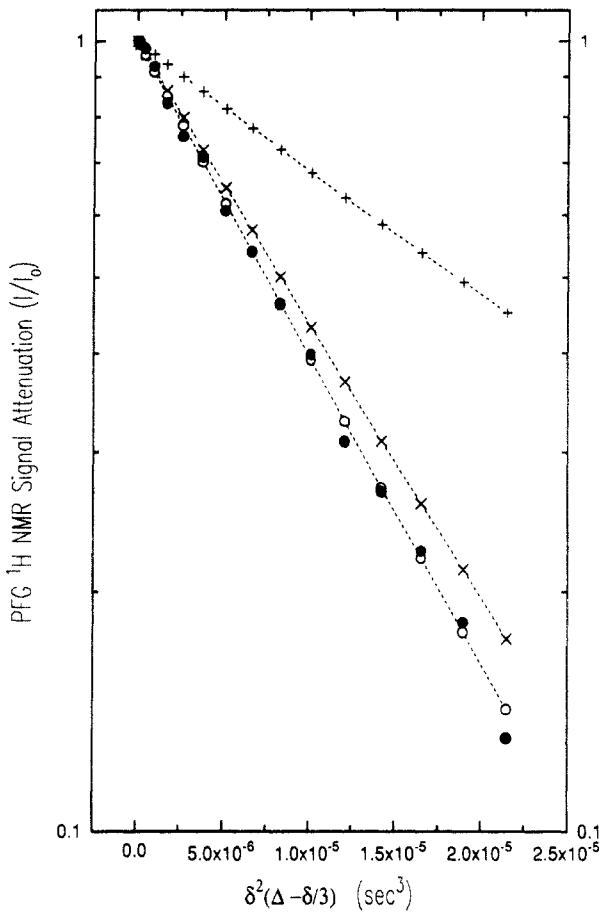

Figure 5. Experimental and calculated PFG NMR data obtained from a "little-delta" experiment for the commercially-available sample of M_5 at $w_p = 0$. Anticipated data were calculated using different scaling laws and a_i values: $D_s(i,w_p=0) \propto MW_i^{-1}$ with the a_i values listed in Table I (+); $D_s(i,w_p=0) \propto MW_i^{-0.5}$ with all values for $a_i = 1$ (×); and for $D_s(i,w_p=0) \propto MW_i^{-0.5}$ with the a_i values listed in Table I (○). Experimental data (●) were obtained using the same Δ, δ, and G values as the calculated data (all three sets) and result in a value of $\langle D_s(5,w_p=0)\rangle = 9.1 \times 10^{-10}$ m^2 s^{-1}.

to i and it scales according to

$$D_s(i,w_p) = \frac{D_s(1,w_p)\,X_c}{i^2} \tag{10}$$

with X_c related to the volume fraction of polymer, ϕ_p, by

$$X_c = X_c^{\circ}/\phi_p \tag{11}$$

Fitting rate equations to the results of styrene over the w_p range 0.5–0.75 suggested that $X_c^{\circ} = 4$ at 50 °C.[6] Equations 9–11 do not indicate how the dependence of D_s on $MW^{-0.5}$ changes to a dependence of MW^{-1} above c^*. Of course, the sharp change in scaling implicit in eq 9–11 is not expected to be a true representation of the experimental data. As the mechanism changes from one dependence to another, it is expected that the change in scaling would be gradual over, say, at least a few monomer units. Moreover, phenomenologically one might expect that over some finite range of w_p each mechanism should dominate before changing to the next mechanism for a finite range of MW.

To test the scaling $D_s \propto MW^{-1}$, it is assumed that the single, average molecular weight of 500 is adequate to describe M_5 up to at least $w_p = 0.6$. If this scaling law were an adequate representation of the data, curves $D_s(2,w_p)$ and $D_s(5,w_p)$ should be parallel to that of $D_s(1,w_p)$ in Figure 3, and they would be lower than $D_s(1,w_p)$ by relative values that are 78/226 and 78/500 times as large for M_2 and M_5, respectively. Close inspection of Figure 3 shows that this is not the case, even within the experimental error of the data, for M_1, M_2, and M_5. The curvature is different for each of the lines: the downward curvature of the data for each of the oligomers is more pronounced in the order $M_5 > M_2 > M_1$. This increase in the vertical spacing of $D_s(i,w_p)$ at a given w_p undermines the simple dependence of $D_s \propto MW^{-1}$, assuming that these relationships hold for small oligomers at such low values of w_p, and ignoring the accepted number for X_c°. Therefore, the general form of the scaling law of eq 9 and 10 is inadequate to describe the data since experimentally there still exists a dependence on w_p.

von Meerwall and co-workers[26,27] have pointed out the importance of considering the effects of the total friction coefficient for a molecule in solution, ζ, defined as

$$\zeta = kT/D_s \tag{13}$$

when testing currently accepted scaling theories for polymer diffusion. For a polymer of degree of polymerization i, its monomeric friction coefficient ζ_1 has been defined simply as[27]

$$\zeta_1 = \zeta_i/i \tag{14}$$

where ζ_i is the friction coefficient for the entire polymer chain. In a series of elegant experiments designed to investigate the interrelationships between probe, solvent, and polymer diffusion, von Meerwall *et al.*[27] were able to "correct" the D_s values of the polymers for the effects of ζ from the probe and show that, for large MW PS molecules (MWs from 10000 to over 1×10^6), current scaling dependencies of D_s on polymer concentration, c, were conformed to. Furthermore, the authors were able to show an adherance of the data to eq 14, and hence identical dependencies of ζ_1 on c, for the different polymer MWs.

In our experiments, however, all solution variables (temperature, matrix polymer, solvent, etc.) have been kept constant and only the degree of polymerization of our probe varied. Consequently, there is no need to correct the D_s values for each probe for changes in the polymer friction coefficient as von Meerwall and co-workers[27] have done. Furthermore, any analyses in terms of ζ values, calculated from the experimentally determined $D_s(i,w_p)$ values, have been avoided since eqs 13 and 14 are most useful if D_s were to scale as MW^{-1}. The implicit assumption in doing this is that the changes in ζ_1 with w_p are incorporated in $D_s(1,w_p)$ and that our probes belong to the same homologous series of compounds. The first of these assumptions seems reasonable given the results of von Meerwall and co-workers,[27] while the second is less tangible and much harder to test, and questions how well our probe molecules act in modeling "true" oligomers of PS.

Values of D_s for M_1, M_2, and M_5 for $w_p > 0$ have been interpolated at several values of w_p from Figure 3 and have been plotted in Figure 6 against the molecular weight of the respective probe molecules. An exponential dependence of $D_s(i,w_p) \propto MW^{-\alpha}$ is assumed, where α is allowed to be a function of w_p. Values of α used are listed in Table II. Further analysis of α as a function of w_p is shown in Figure 7, thus leading to the relationship:

$$D_s(i,w_p) = D_s(1,w_p)\left[\frac{MW_i}{MW_1}\right]^{-(0.49\pm0.05)-(1.75\pm0.14)w_p} \tag{15}$$

for $0 \le w_p \le 0.6$.

Equations 9–11 are based on the assumption that as the diffusing molecule reaches a critical length, a length which depends on the amount of polymer present, its rate of diffusion becomes more sensitive to its molecular weight. In other words, this change may be either gradual or sudden, and its uncertainty lies in the interpretation of the mathematical theory. The experimental results pre-

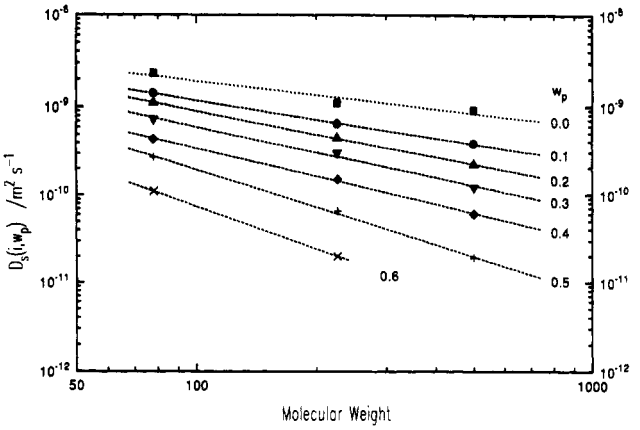

Figure 6. Plot of $D_s(i,w_p)$ versus MW$_i$ for several values of w_p. Data were interpolated from the data in Figure 3. Dotted lines are fitted curves from which values of α have been obtained and listed in Table II. Uncertainty in each $D_s(i,w_p)$ value is approximately ±10%.

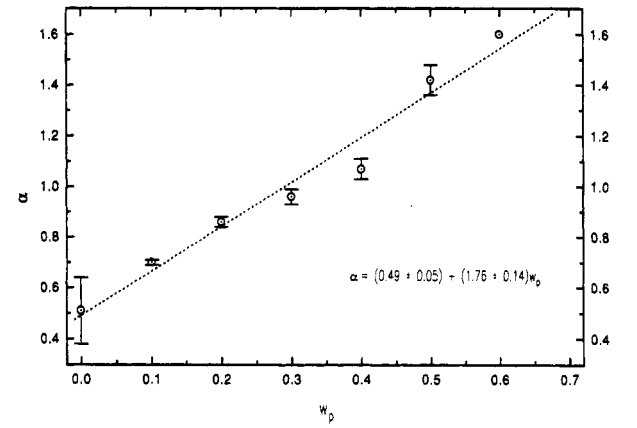

Figure 7. Dependence of α on w_p. The results of a first-order fit are reported in the figure.

Table II. Power-Law Dependence of $D_s(i,w_p)$ on MW$^{-\alpha}$

w_p	α	w_p	α
0.0	0.51 ± 0.13	0.4	1.07 ± 0.04
0.1	0.70 ± 0.01	0.5	1.42 ± 0.06
0.2	0.86 ± 0.02	0.6	1.60
0.3	0.96 ± 0.09		

sented here are inconsistent with expressions 9–11 in two important respects. First, the expressions cannot reconcile powers of less than 1 and noninteger values between 1 and 2. Second, the changes in scaling law increase in a gradual fashion over the entire range of w_p and hence do not show one region where the behavior is given by MW^{-1} and another distinct region where it is dominated by MW^{-2}. The fact that more than one mechanism is operative (interpreted from intermediate values of α) for the diffusion of M_2, even at low w_p, suggests that $X_c°$ must be less than unity for PS if eqs 9–11 are correct. This challenges the previous concept of a critical length, particularly one of several monomer units in length.

The present work is not the first to challenge previously accepted scaling laws. At one extreme the dependence is expressed as $D_s \propto$ MW^{-2}, but this law has been disputed for large MW.[28] The dependence of $D_s \propto i^{-2}$ was originally derived by de Gennes[29-31] for the reptative diffusion of a very large macromolecule within a cross-linked matrix, in which the entanglements are essentially fixed. However, since $X_c° = 4$ at $w_p = 1.0$ has been previously estimated for PS,[6] the onset of the higher power law should not be observed for oligomers $i \leq 5$ at $w_p < 0.8$ on the basis of eqs 9–11. In principle, our work tested neither the validity of the scaling law $D_s \propto$ MW^{-2} nor the point at which the scaling law is predicted to change from a dependence of MW^{-1} to MW^{-2}. Given the present results it appears that the change is gradual rather than abrupt and, in general, the exponent of MW depends on w_p.

Conclusions

Values of the self-diffusion coefficient of model compounds of oligomers of PS, in solutions containing large MW PS, were determined experimentally using PFG NMR. By use of these results, simple scaling laws for the dependence of the self-diffusion coefficients on w_p and on the MW of the oligomers were tested. From our data it appears that the diffusion behavior of samples of benzene/PS containing either M_2 or M_5 does not conform to the simple MW^{-1} scaling law for $w_p \leq 0.6$ and $i \leq 5$. Furthermore, it has been interpreted that a continuously increasing negative exponent in the scaling law may in fact be operative throughout the entire range of MW (and w_p). These general observations should be applicable to modeling free-radical kinetics as well as in predicting the final MWD of polymerizing systems.

Acknowledgment. Donald H. Napper, Alison J. Lennon, Bradley R. Morrison, and Brendan S. Casey are thanked for their thoughtful discussions. The Australian Research Council and National Health and Medical Research Council are also thanked for funding this project.

References and Notes

(1) Schultz, G. V. *Z. Phys. Chem. (Frankfurt am Main)* **1956**, *8*, 290.
(2) Gardon, J. L. *J. Polym. Sci., Part A-1* **1968**, *6*, 2853.
(3) Russell, G. T.; Napper, D. H.; Gilbert, R. G. *Macromolecules* **1988**, *21*, 2133.
(4) Strukelj, M.; Martinho, J. M. G.; Winnik, M. A. *Macromolecules* **1991**, *24*, 2488.
(5) Faldi, A.; Tirrell, M.; Lodge, T. P.; von Meerwall, E. D. *Polym. Prepr. (ACS, Div. Polym. Chem.)* **1991**, *32*, 400.
(6) Russell, G. T.; Gilbert, R. G.; Napper, D. H. *Macromolecules* **1992**, *25*, 2459.
(7) Russell, G. T. Ph.D. Thesis, Sydney, 1990.
(8) Tirrell, M. *Rubber Chem. Technol.* **1984**, *57*, 523.
(9) Walden, P. *Elektrochem. Z.* **1906**, *12*, 77.
(10) Amin Sanayei, R.; O'Driscoll, K. F. *J. Macromol. Sci., Chem.* **1991**, *A28*, 987.
(11) Kosfeld, R.; Goffloo, K. *Kolloid Z. Z. Polym.* **1971**, *247*, 801.
(12) Kosfeld, R.; Schlegel, J. *Angew. Makromol. Chem.* **1973**, *29/30*, 105.
(13) Pickup, S.; Blum, F. D. *Macromolecules* **1989**, *22*, 3961.
(14) Faldi, A. Personal communication.
(15) Callaghan, P. T. *Aust. J. Phys.* **1984**, *37*, 359.
(16) Stilbs, P. *Prog. Nucl. Magn. Reson. Spectrosc.* **1987**, *19*, 1.
(17) Stejskal, E. O.; Tanner, J. E. *J. Chem. Phys.* **1965**, *42*, 288.
(18) Kuchel, P. W.; Chapman, B. E. *J. Magn. Reson.* **1991**, *94*, 574.
(19) Gibbs, S. J.; Johnson, C. S. *J. Magn. Reson.* **1991**, *93*, 395.
(20) Hrovat, M. I.; Wade, C. G. *J. Magn. Reson.* **1981**, *44*, 62.
(21) Mills, R. *J. Phys. Chem.* **1973**, *77*, 685.
(22) Polson, A. *J. Phys. Chem.* **1950**, *54*, 649.
(23) Longsworth, L. G. *J. Am. Chem. Soc.* **1953**, *75*, 5705.
(24) Pascal, P. Ph.D. thesis, Sydney, 1992.
(25) Bueche, F. *Physical Properties of Polymers*; Interscience: New York, 1962.
(26) von Meerwal, E. D. *Rubber Chem. Technol.* **1985**, *3*, 527.
(27) von Meerwall, E. D.; Amis, E. J.; Ferry, J. D. *Macromolecules* **1985**, *18*, 260.
(28) Wheeler, L. M.; Lodge, T. P.; Hanley, B.; Tirrell, M. *Macromolecules* **1987**, *20*, 1120.
(29) de Gennes, P. G. *J. Chem. Phys.* **1971**, *55*, 572.
(30) de Gennes, P. G. *Macromolecules* **1976**, *9*, 594.
(31) de Gennes, P. G. *Macromolecules* **1976**, *9*, 587.